

RESEARCH ARTICLE

Fuel combustion characteristics of aircraft engine main combustion chamber based on kerosene ignition

Jing Liu*, Shuai Liu, Yi Ding, Lina Liu

School of Mechanical and Electrical Engineering, Huanghe Jiaotong University, Jiaozuo, Henan, China.

Received: May 27, 2024; accepted: August 3, 2024.

As the aviation industry develops quickly, the demand for low fuel consumption and high clean energy of aircraft engines is more prominent. So far, for aviation kerosene used in aircraft engines, the detailed combustion reaction mechanism and chemical reactions in combustion chamber are not clear. In response to the above problems, this study investigated the simplified reaction mechanism of the fuel during combustion simulation by analyzing the combustion characteristics of a domestic aviation kerosene. The results indicated that, if the initial temperature of the mixed gas was the same, under different pressure states, the laminar combustion velocity of aviation kerosene increased with the raise of pressure. The laminar combustion velocity was closer to the experimental value under the semi-detailed mechanism calculation. Therefore, the simplified model proposed in this study was both feasible and effective, which could be utilized to analyze the combustion characteristics of fuel in the combustion chamber of aviation engines based on kerosene ignition.

Keywords: fuel combustion; aircraft engine; kerosene; ignition; fuel consumption; clean energy.

*Corresponding author: Jing Liu, School of Mechanical and Electrical Engineering, Huanghe Jiaotong University, Jiaozuo 454000, Henan, China. Email: liujing2024lj@163.com.

Introduction

As the progress of economy and society, the aviation industry has developed rapidly. The number of flights has continued to increase. The resulting aviation pollutant emission problem is becoming more severe [1, 2]. For a jet engine's primary combustion chamber (CC), the mixing, ignition, and combustion of fuel is a complex erratic mixing. During the reaction, many intermediate products such as free radicals, atoms, and ions are produced. They are closely related to the ignition of fuel, combustion efficiency, flame structure, flame stability, formation of combustion pollutants, and thrust of aviation engines [3, 4]. To ensure the excellent

performance of the core engine, the main CC must have good combustion stability. Therefore, the studies of combustion characteristics such as fuel ignition, flame morphology, flame propagation, extinction boundary, and combustion limit are the keys and difficult points in the development of CCs. Aviation kerosene is a hydrocarbon mixture fuel composed of hundreds of components, including various chain hydrocarbons, cycloalkanes, and aromatic compounds. At this stage, there are still many deficiencies in the research of these compounds [5].

With the gradual advancement of the sustainable development strategy, the development and

utilization of various clean aviation energy sources has become a research hotspot. Focusing on the challenge of numerical simulation of the deflagration-to-detonation transition (DDT) process in the combustion of aviation kerosene, Huang *et al.* proposed the aviation kerosene's single-component simplification mechanism and carried out numerical modeling on the DDT process. The findings demonstrated that the single-component alternative fuel's simpler mechanism model could more accurately predict how aviation kerosene would burn at high temperatures and pressures [6]. Liu *et al.* aimed at the change of flame propagation characteristics, while aviation kerosene was burning caused by the low pressure. The burning velocity was measured under different initial pressure, temperature, and equivalence ratio. The results indicated that it was more challenging to ignite the fuel at situations with lower pressures of 25 kPa and lower temperatures of 420 K. At the same low pressure of 25 kPa, the two particular reactions had very little of a detrimental effect on the laminar combustion speed [7]. Sun *et al.* performed a comparison study on the soot premise and accumulation characteristics of algae biofuel and aviation kerosene RP-3 in a laminar flame to explore reasons for the less soot formation of biofuels. The results showed that the biofuels produced less soot, which weakened the nucleation and growth of soot [8]. Ming and Yang undertook a test-driven investigation on the behavior characteristics of the droplets occurring inside and on the droplet interface of burning aviation kerosene. The results demonstrated that the internal flow was significantly impacted by the Marangoni effect. The capillary wave's amplitude was not constant on the droplet's surface, showing the characteristics of amplitude ranging from 110 μm to 120 μm [9]. Woortman *et al.* investigated the effect of synthetic analogs of aromatic carotenoid cleavage products on jet fuel combustion properties, compared free radical scavenging and endothelial cell culture cytotoxicity. Reduced non-renewable consumption was achieved by using aromatic

carotenoid cleavage products as antioxidants [10].

Pollutants emitted by aircraft engines can cause serious harm to human beings and the ecological environment. It has significant scientific implications to study the detailed emission data of key chemical components and carbon particles from aircraft engines. Fei *et al.* designed a new type of integrated afterburner by adopting the overall structure of combined strut-cavity-injector. The results indicated that the combination of strut-cavity-injector could achieve consistent combustion. Plasma ignition could enhance the properties of ignition. Moreover, plasma ignition resulted in a 67 ms reduction in ignition delay time compared to traditional spark ignition. In addition, by raising intake air velocity and decreasing the surplus air ratio, the ignition delay time was decreased [11]. Wang *et al.* developed ever-increasing new technologies such as turbocharging, variable valve actuation (VVA), and exhaust gas recirculation (EGR) to fulfill the demanding fuel efficiency and pollution standards for spark ignition engines. The findings showed that the most notable impact on it came from EGR rate, which effectively improved the anti-knock performance when the optimized parameters were applied [12]. Depending on the results of the intricate reaction flow field structure in the CC of an aircraft engine, Zhang *et al.* established a thorough model of the chemical reactor network to accurately predict the nitrogen oxide and carbon monoxide (CO) emissions of advanced civil aircraft engines. It was found that the complicated chemical reactor network model's forecast for NO_x emissions were in the best agreement with those obtained using empirical formulas [13]. Khodayari *et al.* used computational fluid dynamics (CFD) chemical reactor network (CFD-CRN) approach to predict pollutant emissions from aeroengine combustors by simulating combustion in highly swirling flows. Experimental results proved that the accuracy of pollutant emissions simulated by this method was high [14]. Wang *et al.* used optical diagnostics to obtain NO and OH

chemiluminescence images of separated stratified rotating spray flames in NO_x emission measurements. The results demonstrated that the main flame and pilot flame were only weakly connected, and NO_x emission rose as fuel grade ratio increases. Due to the pilot flame's high adiabatic flame temperature, it was crucial in the production of NO_x emissions [15].

Although many studies have examined the combustion characteristics of aviation kerosene and fuel in aircraft engine CC, there is still a lack of research on the detailed chemical changes and combustion mechanisms under multiple operating conditions. This study addressed this gap by investigating the combustion characteristics of domestically produced aviation kerosene, analyzing the combustion efficiency, emission generation, and stability mechanisms of the fuel. The objective of this research was to develop an accurate and applicable reaction kinetics model for aviation kerosene that better described the chemical reactions in the CC. This research combined CFD with a simplified reaction mechanism model to simulate and validate the combustion and emission characteristics. The results of this study would be useful to predict and optimize combustion processes in aircraft engine CCs, thereby reducing pollutant emissions and improving efficiency. Furthermore, it would have important implications for advancing scientific understanding and technological development in this field.

Materials and methods

Choice of aviation kerosene characterization fuel

In the combustion process of aviation fuel, the actual fuel is affected by different factors including temperature and pressure, making the combustion process more complex. Aviation kerosene is a hydrocarbon fuel with complex and diverse components [16, 17], and was analyzed in the jet-stirred reactor (JSR) in this research with the main characterizations (Table 1) [18, 19]. The major ingredients of aviation kerosene fuels are

n-dodecane, n-undecane, and n-nonane. n-decane fuel is a primary ingredient of aviation kerosene and main characteristic fuel for aviation engines, which has the most similar physical and chemical properties to aviation kerosene, and therefore, was used as a characterization fuel for the engine of a domestic aviation aircraft model in this research to investigate the fuel combustion reaction mechanism.

Mechanism verification of aviation characterization of fuel combustion reactions

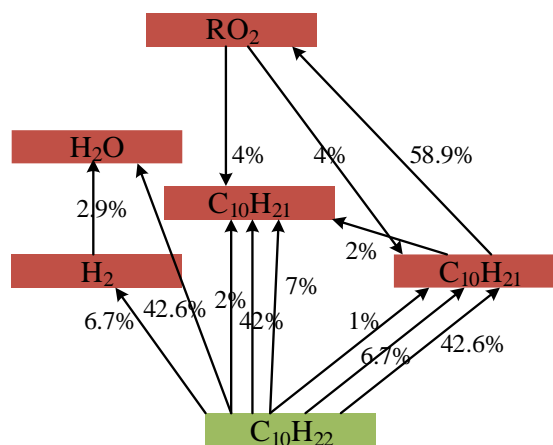
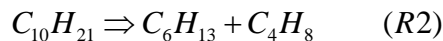
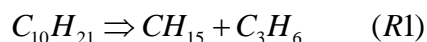
Based on the reaction principle of n-decane ignition and combustion, the main reaction factors characterizing the fuel were studied. n-decane is a flammable liquid that can undergo strong chemical reactions with oxidants. Considering the enhancements to the combustion reaction mechanism proposed by Suzuki *et al.* [20], an in-depth examination was conducted on the primary pre-factors to ascertain the combustion chemical reaction characteristics of n-decane. The key reactions characterized the decomposition and oxidation of fuel after heating included decomposition into a decyl radical and a hydrogen atom when exposed to high temperatures, which marked the beginning of the combustion process. Then the decyl radical reacted with molecular oxygen to form a decane and a hydroperoxy radical, which was a crucial step for the propagation of combustion. The further oxidation of decane would produce another decyl radical and hydroperoxy radical, which continued the chain reaction necessary for sustained combustion [21, 22]. In subsequent reactions, the newly formed decyl radical underwent additional oxidation, forming decyne and another hydroperoxy radical. This process contributed significantly to the overall energy release observed during combustion. The decyne was then broken down into smaller molecules such as ethylene, ethyl radical, acetylene, and CO. These smaller molecules served as essential intermediates in the complete combustion of n-decane. The primary reaction pathways of n-decane were examined based on the observed reaction steps when the system was comprised of a mixture of

Table 1. The candidate surrogates of kerosene.

Test fuel	Characterize fuel	Reaction mechanism	Experimental environment
Jet A-1	78% n-decane 12.2% toluene 9.8% cyclohexane	188 components; 1,463 reactions	JSR
Jet A-1	n-decane	78 components; 603 reactions	JSR
Jet A-1	74% n-decane 11% n-propylcyclohexane 15% n-propylbenzene	207 components; 1,592 reactions	JSR
JP-8	32.6% n-decane 34.7% n-dodecane n-propylcyclohexane 16% n-butylbenzene 16.7% methylcyclohexane	164 components; 1,162 reactions	JSR
Jet A-1	70% n-decane 30% n-propylbenzene	300 components; 1600 reactions	shock tube

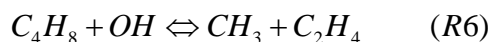
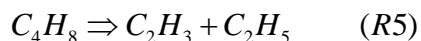
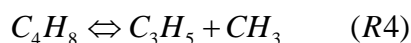
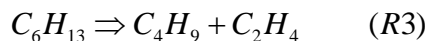
n-decane and air with a volume ratio of 1:2, a pressure of 0.1 MPa, and temperatures of 700 K and 1,100 K (Figure 1). The hydrogen-oxygen reaction was the main consumption path of n-decane. When the temperature conditions were 700 K and 1,100 K, after consumption of n-decane ($C_{10}H_{22}$), $C_{10}H_{21}$ decane was generated. During the formation of decane, hydroxide (OH) was the most active radical followed by oxygen molecules [23]. When the ratio of n-decane to air mixture was 1.0, the pressure was 0.1 MPa, and the temperature was 700 K, the oxidation reaction of the above two decyl groups was relatively slow. Then, peroxyalkyl groups including SXRO2 and TXRO2 were formed and subsequently oxidized to form peroxyhydroalkyl groups such as T2O2R02H. At the medium temperature, n-decane exhibited obvious negative temperature coefficient (NTC) characteristics. As the temperature increased, it became even more difficult for the fuel to ignite. The combustion speed slowed down, and the ignition delay period increased. The tetraoxohydroalkyl group was decomposed into small molecules through two-step reactions including ethyl (C_2H_5), ethylene (C_2H_4), formaldehyde (CH_2O), and CO. The hydroxyl groups (OH) required for chain reaction initiation were also produced in large quantities. The combustion of n-decane was converted into a

rapid oxidation stage of small molecules [24, 25]. Under high temperature conditions, the hydrogen oxygen reaction generated a decane group and then split into olefins and decane groups with the specific components below.

**Figure 1.** Analysis of reaction pathways of characterization fuels under different mixture ratios and different temperatures.

Some olefins and alkane groups continued to undergo cracking reactions to produce small molecules such as olefins and alkanes. The other

part reacted with highly oxidizing elements such as OH radicals and oxygen free radicals (O), continuing to decompose into smaller molecules as shown below [26].



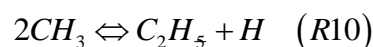
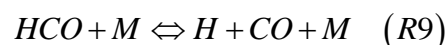
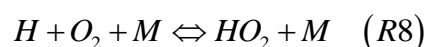
Through the above reaction mechanism, the calculation of the fuel characteristics during the fuel ignition process was completed by a selected domestic aviation aircraft. The reaction rate of fuel combustion was shown in formula (1).

$$k = AT^b \exp\left(-\frac{E}{RT}\right) \quad (1)$$

where k was the constant of the reaction rate. A was the pre-exponential factor. T was the temperature. b was the temperature index. E was the activation performance of the fuel. R was the general constant of the gas. Based on the reaction mechanism and combustion reaction of the fuel, the parameters A and b were adjusted to optimize the reaction rate of fuel combustion and improve the reaction mechanism. In the optimization process, the first thing to consider was the ignition characteristics of the fuel. Since temperature had the greatest effect on the rate of ignition, the principle of adjusting ignition characteristics mainly considered temperature factors. The elementary reaction with the greatest influence on the ignition characteristics at different temperature ranges was then determined. Through sensitivity analysis of operating conditions at temperatures ranging from 1,100 to 1,600 K, equivalence ratio of 1.0, and pressure of 0.1 MPa, multiple attempts were made to adjust the pre-exponential factor of the reaction with the goal of ignition delay time. The appropriate pre-index factor was determined and the reaction characteristics of n-decane were shown below.



After determining the pre-exponential factor, the flame propagation speed should be considered as another influencing factor. In the range of equivalence ratio, the elementary reaction that had a greater impact on the fuel flame propagation speed was determined. The elementary reaction had little effect on the flame delay characteristics. The three most suitable elementary reactions (R8, R9, R10) were shown below.



The different numbered R indicated the specific chemical reaction steps of n-decane under different conditions. The utilization of these numbers served to distinguish and identify the discrete chemical reaction steps, thereby facilitating enhanced clarity when analyzing and describing the combustion mechanism. Specifically, R1 to R7 were the various reaction steps of n-decane under different temperature and pressure conditions. R8, R9, and R10 were three reaction steps with special emphasis and had a great influence on the speed of fuel flame propagation.

Construction of aviation kerosene fuel reaction model based on CFD

Based on the above reaction mechanism, the emissions from fuel combustion were numerically simulated. With the increase of the total number of elementary reactions of fuel combustion, the required calculation capacity increased [27]. The CC of an aircraft engine was formed by a flame tube, an exterior inner and outer casing, a diffuser, and a connecting pipe. Under the ideal state of the CC flame tube, the calculation for the state of gas was shown in formula (2).

$$P = \rho RT \quad (2)$$

where P was the pressure. ρ was the density of the mixed gas in the CC. R was the general constant of the gas. T was the temperature of the mixed gas in the CC. The calculation method under the state of mass balance in the CC was shown in formula (3).

$$\frac{\partial \rho}{\partial t} + \frac{\partial(\rho u_i)}{\partial x_i} = 0 \quad (3)$$

where t was the burning time. x_i was the parameter in the rectangular coordinate system. u_i was the speed in the i direction of the rectangular coordinate system. The calculation method for momentum balance was shown in formula (4).

$$\frac{\partial(\rho u_i)}{\partial t} + \frac{\partial \rho u_i u_j}{\partial x_j} = -\frac{\partial P}{\partial x_i} + \frac{\partial \sigma_{ij}}{\partial x_j} \quad (4)$$

where i and j were the direction of the coordinate axis. u_i was the velocity in the i direction. u_j was the velocity in the j direction. σ_{ij} was the viscous stress tensor. x_i and x_j were parameters of rectangular coordinate system. The standard u_i double equation turbulence model was used to calculate the flowing gas in the CC. The calculation for u_i after decomposition and simplification was shown in formula (5).

$$\rho \frac{Dk}{Dt} = \frac{\partial}{\partial x_j} \left(\frac{\mu_t}{\sigma_k} \frac{\partial k}{\partial x_j} \right) + \mu_1 \frac{\varepsilon}{k} \mu_1 \left(\frac{\partial v_i}{\partial x_j} + \frac{\partial v_j}{\partial x_i} \right) \frac{\partial v_i}{\partial x_j} - \rho C_D \varepsilon \quad (5)$$

where C_1 was a constant with a value of 1.44. σ_ε was the Prandtl function of the dissipation rate of pulsating kinetic energy ε , which was usually with a value of 1.3. σ_k was the effective Prandtl function of the diffusion of turbulent pulsating kinetic energy k , which was usually with a constant 0.09. The value of C_D was

usually 1.0. Dt was the combustion time of component D . The calculation of ε was shown in formula (12).

$$\rho \frac{D\varepsilon}{Dt} = \frac{\partial}{\partial x_j} \left(\frac{\mu_t}{\sigma_\varepsilon} \frac{\partial \varepsilon}{\partial x_j} \right) + C_1 \frac{\varepsilon}{k} \mu_1 \left(\frac{\partial v_i}{\partial x_j} + \frac{\partial v_j}{\partial x_i} \right) \frac{\partial v_i}{\partial x_j} - C_2 \rho \frac{\varepsilon^2}{k} \quad (6)$$

where C_1 and C_2 are constants. In the eddy dissipation model, the generation rate $R_{i,r}$ of the i -th substance generated by the r -th component could be obtained. The calculation of $R_{i,r}$ was shown in formula (7).

$$R_{i,r} = v_{i,r}^m M_{w,i} A B \rho \frac{\varepsilon}{k} \frac{\sum P Y_P}{\sum_j v_{i,r}^m M_{w,j}} \quad (7)$$

where Y_P was the mass fraction of P . A and B were empirical constants. The conceptual model of eddy dissipation indicated that the chemical reaction occurred in a well-scaled vortex. In the well-scaled range, the fuel was considered to participate in the chemical reaction [28]. The calculation for good scale vortex volume fraction ζ^* was shown in formula (8).

$$\zeta^* = C_\zeta \left(\frac{V\varepsilon}{k^2} \right)^{3/4} \quad (8)$$

where ζ^* was the constant of volume fraction. The calculation of scale time τ^* was shown in formula (9).

$$\tau^* = C_\tau \left(\frac{V}{\varepsilon} \right)^{1/2} \quad (9)$$

where C_τ was the constant of the time scale. As an extension of the eddy dissipation model, the eddy dissipation conceptual model took into account the survival time of turbulent vortex and the time required for reaction, including the dual effects of turbulent flow and detailed

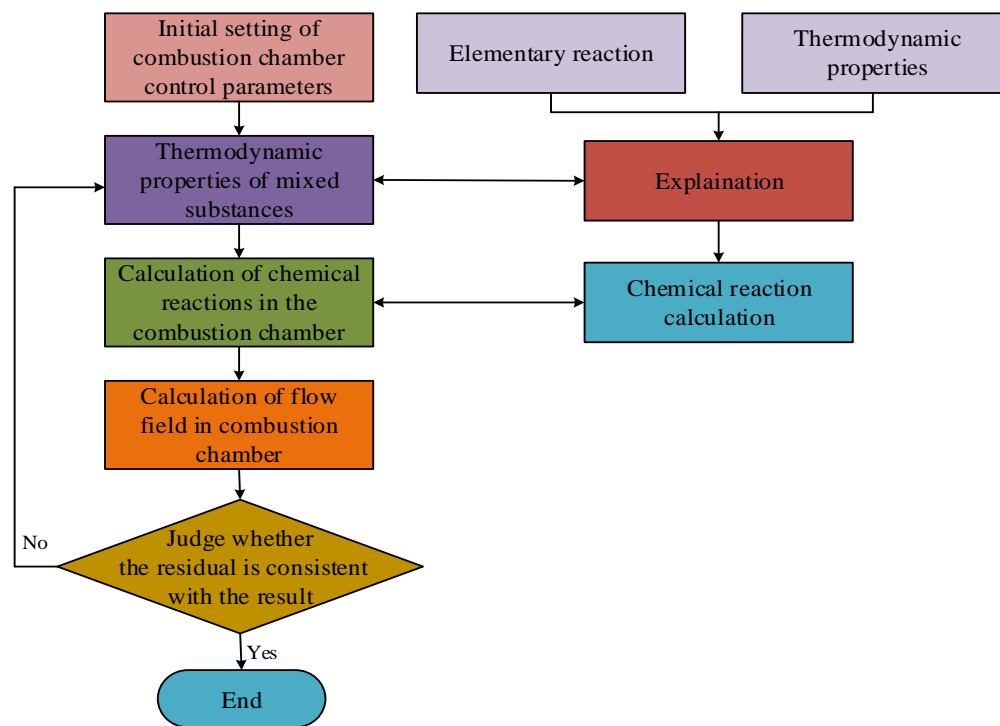


Figure 2. Schematic of reaction mechanism combined with CFD.

combustion reaction model.

The study employed CFD software (<https://www.ansys.com/products/fluids/ansys-fluent>) combined with a simplified reaction mechanism model to simulate and experimentally validate the combustion and emission characteristics of aviation kerosene (Figure 2). The combustion emission characteristics were coupled through CFD software. The temperature changes, reactants, final products, intermediate products, and concentrations of pollutants in the CC of the aircraft engine could be determined for various chemical combustion reaction characteristics. The data used for constructing the proposed model were sourced from the National Institute of Standards and Technology (NIST) (Gaithersburg, Maryland, USA). The dataset included detailed combustion reaction mechanisms, properties of n-decane, and other hydrocarbons. The dataset consisted of 10,000 data points and was collected in 2021, which included experimental measurements of ignition

delay times, laminar flame speeds, and emission profiles under various conditions. 70% of the data was used for training the model, while the remaining 30% was used for testing and validation.

Results and discussion

Reaction mechanism in engine combustion chamber

The reaction mechanism of a certain aviation kerosene after combustion were selected as the experimental data for calculation. CH_4 and C_2H_2 cracking products were selected from various cracking products for rate of production (ROP) analysis. In a certain combustion reactor, numerical calculation method was used to evaluate the contribution of elementary reaction to the generation or consumption of reaction components. The main reaction process in the overall reaction was then obtained. Each elementary reaction contained different components, which had a direct or indirect

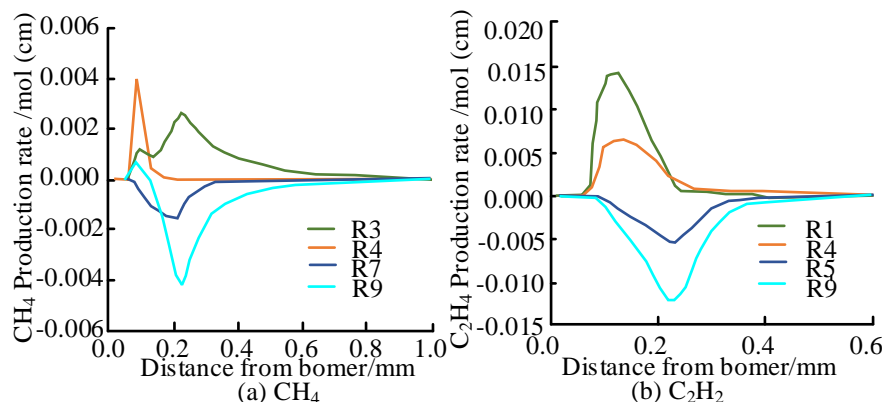


Figure 3. Production and consumption rate of the pyrolysis.

impact on the final product. Therefore, ROP was used to analyze the products after combustion to better analyze the emissions in the CC. The ROP diagram of the main elementary reactions of CH₄ and C₂H₂ in the combustion process of n-decane was shown in Figure 3. The results showed that R9 elementary reaction had the greatest impact on the generation and consumption of CH₄ followed by the elementary reaction of R4, R3, and R7, respectively. The generation and consumption rate of CH₄ reached 0.0145 mol/cm³·s (Figure 3a). R1, R4, R5, and R9 were the main elementary reaction of C₂H₂. Among them, R9 elementary reaction had the greatest impact on the production and consumption of C₂H₄. The generation and consumption rate of C₂H₄ was 0.0233 mol/cm³·s (Figure 3b). The results suggested that the influence of elementary reaction of small molecular substances on various substances in the CC should be fully considered in the combustion process of aviation kerosene fuel.

Various chemical reactions in the CC were complex and varied. To enhance the characteristics of the CC and deal with various actual situations, it was necessary to calculate the process and results of various chemical combustion in the CC in detail. However, the related calculation was large and complex. Therefore, the simplified mechanism proposed in this study was used for calculation. The ignition characteristics of aviation kerosene based on

semi detailed mechanisms were used as a comparative method. The results showed that, when the pressure was 0.1 MPa and the equivalence ratio was 0.5, the ignition delay time calculated by the simplified mechanism was slightly higher than that of the aviation kerosene used in the study. The result was closer to the effect of aviation kerosene used in the research, which was better than the semi-detailed mechanism. When the initial pressure of the gas mixture was 0.1 MPa and the equivalence ratio was 1, the ignition delay time calculated by the simplified mechanism takes longer at high temperature, which was closer to the experimental value at low temperature. As the initial pressure raised to 0.2 MPa, the simplified mechanism and the detailed mechanism's calculations of the ignition delay time was more consistent with the aviation kerosene used in the study (Figure 4). Overall, the simplified mechanism's calculation of the ignition delay time agreed more closely with the experimental result. The simplified mechanism of the characterization fuel could well demonstrate the ignition characteristics of the aviation kerosene used in the research.

The rate of mixed laminar combustion was greatly affected by temperature and pressure. Figure 5 demonstrated the comparison of the rate of mixed laminar combustion under different temperature and pressure conditions. When the initial temperature of the mixture was

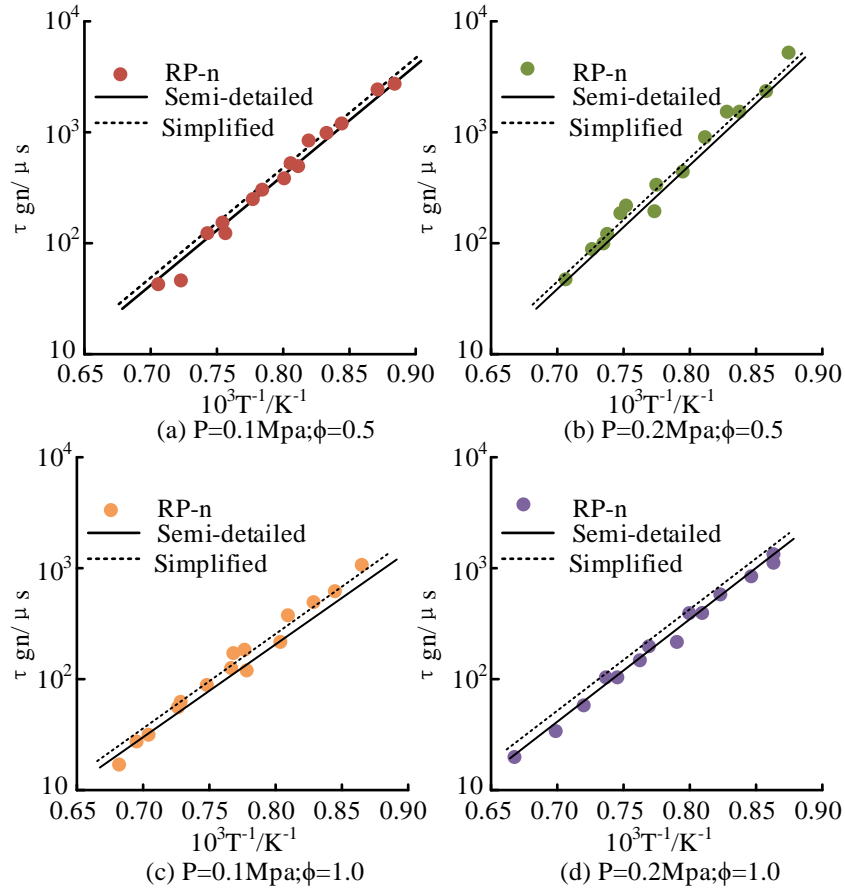


Figure 4. Comparison of ignition delay time of CC under three different fuel mechanisms.

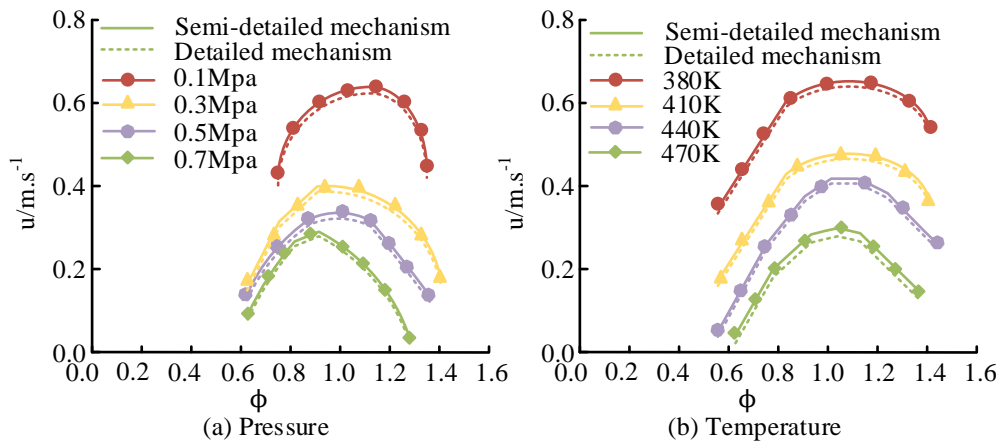


Figure 5. Comparison of combustion speed of CC under different pressure and temperature conditions.

the same, the laminar combustion velocity of aviation kerosene under different pressure conditions increased with increasing pressure. The laminar combustion velocity and semi-

detailed mechanism were more consistent with the experimental values (Figure 5a). When the pressure of the mixed gas was kept at 0.1 MPa, the laminar combustion rate of the mixed gas

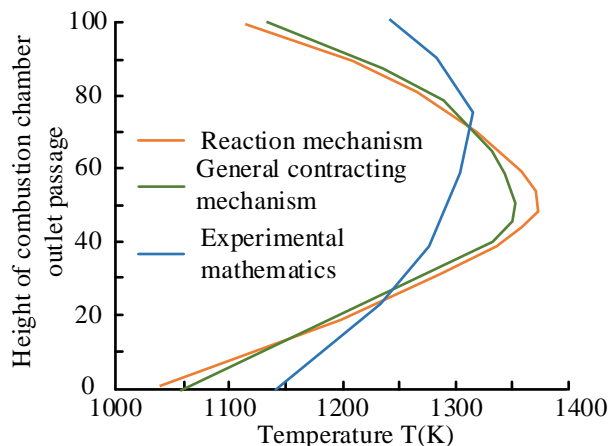


Figure 6. Temperature distribution characteristics of CC outlet.

increased gradually as the starting temperature increased (Figure 5b). The results suggested that the simplified mechanism could basically be used as the chemical reaction kinetics mechanism of aviation kerosene used in the research, which could better demonstrate the basic characteristics of aviation kerosene such as ignition delay characteristics of fuel and laminar combustion rate.

During the combustion of kerosene fuel in the aircraft engine combustor, the temperature at the outlet of the combustor changed greatly due to the influence of the air involved in the combustion. The specific temperature data that was from a certain aviation aircraft group company was used for this study (Figure 6). The results demonstrated a relatively good radial distribution of the CC outlet temperature. The high-temperature zone was distributed above 2/3 of the CC outlet channel. According to the radial distribution of outlet temperature calculated by the simplified mechanism, the temperature of the blade tip was significantly higher than that of the blade root. The temperature was the highest at 45% to 75% of the height of the flame tube outlet, which was consistent with the results of this study. The radial distribution of CC outlet temperature calculated by the simplified mechanism was closer to the experimental data.

Overall, combined with ROP analysis, the reaction mechanism of a certain aviation kerosene characterized fuel was obtained. Through this proposed reaction model, the combustion characteristics of the aviation kerosene were compared and analyzed with semi-detailed and detailed mechanisms. The simplified model was better suited to reflecting the combustion and ignition characteristics of aviation kerosene. Based on the simplified mechanism proposed in the study, the combustion characteristics of fuel under different operating conditions were analyzed in detail.

Analysis of combustion emissions

Aviation kerosene has a significant amount of emissions after combustion in the CC. Through the analysis of the concentration of emissions after fuel combustion, whether the relevant emissions meet the emission standards and environmental requirements after aviation fuel combustion can be better judged, providing corresponding data support for the timely disposal of emissions. The pollutants emitted by aircraft engines mainly include CO₂, soot, etc., as well as a small amount of CO, UHC, NO, and SO. CO₂ and H₂O emissions were selected for analysis in this study. The concentration distribution of CO₂ and H₂O in the combustor flame cylinder was shown in Figure 7. When the simplified mechanism was used for calculation, the

products included CO and CO₂. When the fuel was incompletely burned, the concentration of CO was relatively high. When the fuel was fully burned, CO would continue to be oxidized to CO₂. Therefore, the concentration of CO₂ was relatively high. Due to the relatively small remaining space in the CC and insufficient air supply, aviation kerosene could not be completely oxidized. The concentration of CO produced by combustion was relatively high, and the concentration of CO₂ was relatively low. The higher concentration of CO reflected the reduced heat release, so the gas temperature in this area was lower. Nitrogen oxides are the main pollutants emitted after fuel combustion in the combustor.

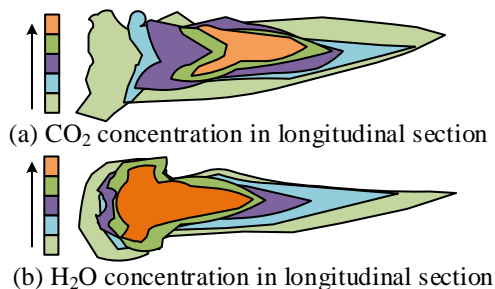


Figure 7. CO₂ and H₂O concentration distribution in CC.

The concentration distribution of NO_x at different positions in the CC was shown in Figure 8. With the progressive rise of the core temperature, a large amount of NO_x gas was emitted, reaching 1,900 ppm. As a large amount of air entered the mixing zone, the temperature of the main combustion zone decreased. NO_x also rapidly decreased. The NO_x at the outlet had dropped below 1,000 ppm. Combining the results of Figures 8a and 8b, the high NO_x emission area in the flame tube was still a high temperature area. From the perspective of the overall distribution of NO_x, the distribution concentration of NO_x was significantly correlated positively with temperature, while the generated NO_x was mainly thermal NO. As the temperature decreased, the concentration of NO also decreased rapidly.

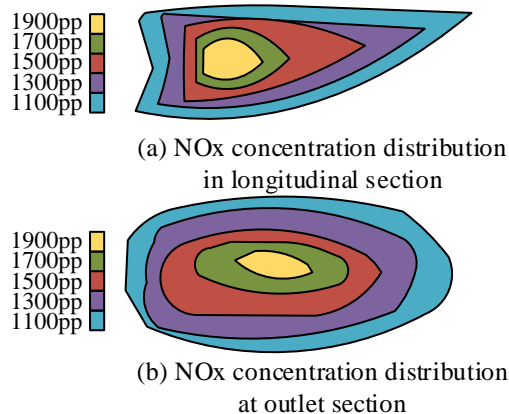


Figure 8. NO_x concentration distribution in CC.

Conclusion

The growth of the aviation industry has led to an increased demand for high-efficiency and clean aviation fuel. This study proposed a simplified reaction mechanism for characterizing fuel based on the ignition and combustion characteristics of a domestic aircraft model, utilizing aviation kerosene as the fuel source. The mechanism, coupled with CFD, was used to explore the combustion and emission characteristics of aviation fuel. The study found that the initial pressure significantly impacted flame development, and the simplified mechanism effectively analyzed the combustion characteristics of aviation kerosene under various operating conditions. The results provided a more accurate prediction of ignition delay and laminar combustion rates compared to semi-detailed mechanisms. Additionally, the emission analysis indicated that incomplete combustion led to higher CO concentrations, while complete combustion resulted in higher CO₂ emissions. NO_x emissions were found to be positively correlated with temperature. The simplified mechanism proposed in this study could effectively predict and optimize combustion processes in aircraft engine combustors, reduce pollutant emissions, and improve combustion efficiency. This research provided valuable insights for advancing scientific understanding and technological

development in the field of aviation fuel combustion.

Acknowledgements

The research was supported by the National Natural Science Foundation of China (Grant No. 52375052).

References

- Paccati S, Bertini D, Mazzei L, Andreini A. 2021. Large-eddy simulation of a model aero-engine sooting flame with a multiphysics approach. *Flow Turbulence Combust.* 106(4):1329-1354.
- Rao KN, Prasad B, Babu CK, Degaonkar GK. 2022. Influence of inlet swirl on pattern factor and pressure loss in an aero engine combustor. *J Mech Eng Sci.* 236(5):2631-2645.
- Agbadede R, Kainga B. 2020. Effect of water injection into aero-derivative gas turbine combustors on NOx reduction. *Eur J Eng Res Sci.* 5(11):1357-1359.
- Zeng H, Wang B, Zou W, Zheng X. 2022. Influence of pressure pulsation on the performance of compression system and turbocharged engine. *J Automob Eng.* 236(5):927-937.
- Li L, Suo J, Yu H, Zhang L. 2020. Optimal design and application of gas analysis system. *J Northwestern Polytech Univ.* 38(1):104-113.
- Huang X, Wang D, Xiao Z, Yu Z. 2022. Numerical simulation of DDT process of aviation kerosene one-component alternative fuel. *J Northwestern Polytech Univ.* 40(3):610-617.
- Liu J, Zhang D, Hou L, Yang J, Xu G. 2022. Laminar burning speed of aviation kerosene at low pressures. *Energies.* 15(6):1-11.
- Sun M, Gan Z, Yang Y. 2021. A comparison study of soot precursor and aggregate property between algae-based aviation biofuel and aviation kerosene RP-3 in laminar flame. *J Energy Resour Technol.* 143(11):1-44.
- Ming HE, Ying P. 2021. An experimental study on the phenomena inside the burning aviation kerosene droplet. *J Therm Sci.* 30(6):2202-2213.
- Woorntman DV, Jürgens S, Untergehrer M, Rechenberger J, Fuchs M, Mehler N, *et al.* 2020. Greener aromatic antioxidants for aviation and beyond. *Sustain Energy Fuels.* 4(5):2153-2163.
- Fei L, Zhao BB, Liu X, He LM, Deng J, Lei JP, *et al.* 2021. Application study on plasma ignition in aeroengine strut-cavity-injector integrated afterburner. *Plasma Sci Technol.* 23(10):186-196.
- Qin H, Tang G, Wang X. 2021. Effects of pressure oscillation on aerodynamic characteristics in an aero-engine combustor. *Chin J Aeronaut.* 2021(2):454-465.
- Zhang Q, Hai H, Li C, Wang Y, Zhang P, Wang X. 2020. Predictions of NOx and CO emissions from a low-emission concentric staged combustor for civil aeroengines. *J Aerosp Eng.* 234(5):1075-1091.
- Khodayari H, Ommi FS, Saboohi Z. 2020. Uncertainty analysis of the chemical reactor network approach for predicting the pollutant emissions in a double swirl combustor. *J Energy Resour Technol.* 142(9):1-22.
- Wang Z, Lin Y, Wang J, Zhang C, Peng Z. 2020. Experimental study on NOx emission correlation of fuel staged combustion in a LPP combustor at high pressure based on NO-chemiluminescence. *Chin J Aeronaut.* 11(2):550-560.
- Li W, Cai W, Duan Z, Di D, Yan Y. 2020. Effect of fuel temperature on the atomization characteristics for swirl injector. *Atomization Sprays.* 30(10):697-711.
- Null LV, Zeng N, Ding N, Weng NY. 2020. Experimental investigation of a novel micro gas turbine with flexible switching function for distributed power system. *Front Energy.* 14(4):790-800.
- Sun J, Shao S, Hu X. 2022. Synthesis of oxygen-containing precursors of aviation fuel via carbonylation of the aqueous bio-oil fraction followed by C-C coupling. *ACS Sustain Chem Eng.* 10(33):11030-11040.
- Boehm RC, Yang Z, Heyne JS. 2022. Threshold sooting index of sustainable aviation fuel candidates from composition input alone: Progress toward uncertainty quantification. *Energy Fuels.* 36(4):1916-1928.
- Suzuki S, Obuchi A, Kukkadapu G, Kinoshita K, Takeda Y, Oguma M, *et al.* 2021. Measurements of intermediate species in fuel-rich oxidation of Ethylene, Toluene, and n-Decane. *Energy Fuels.* 35(18):14924-14940.
- He Z, Peng Y, Jiao Y. 2020. Improved catalytic stability and anti-coking ability of Ni/La₂O₃-Al₂O₃ catalyst by doping alkaline earth metals for n-decane reforming. *Int J Hydrogen Energy.* 45(46):24626-24635.
- Hatab FA, Darwish AS, Lemaoui T, Warrag S, Benguerba Y, Kroon MC, *et al.* 2020. Extraction of thiophene, pyridine, and toluene from n-decane model diesel using betaine-based natural deep eutectic solvents. *J Chem Eng Data.* 65(11):5443-5457.
- Lobakova ES, Dolnikova GA, Ivanova EA, Sanjjeva DA, Dedov AG. 2021. Community of hydrocarbon-oxidizing bacteria in petroleum products on the example of Ts-1 aviation fuel and Ai-95 gasoline. *Biotekhnologiya.* 37(1):54-68.
- Gawron B, Bialecki T, Janicka A, Zawilak M, Corniak A. 2020. Exhaust toxicity evaluation in a gas turbine engine fueled by aviation fuel containing synthesized hydrocarbons. *Aircraft Eng Aerosp Technol.* 92(1):60-66.
- Miller JH, Hafenstine GR, Nguyen HH, Vardon DR. 2022. Kinetics and reactor design principles of volatile fatty acid ketonization for sustainable aviation fuel production. *Ind Eng Chem Res.* 61(8):2997-3010.
- Etuk SE, Emah JB, Robert UW, Agbasi OE, Akpabio IA. 2021. Comparison of electrical resistivity of soots formed by combustion of kerosene, diesel, aviation fuel, and their mixtures. *Brilliant Eng.* 2(3):6-10.
- Rezaee S, Vashahi F, Dafsari RA, Lee J. 2021. A correlation of aviation fuel temperature effect on mean drop size in pressure swirl spray. *Atomization Sprays.* 31(4):81-97.

28. Du C, Han C, Yang Z, Wu H, Luo H, Niedzwiecki L, *et al.* 2022. Multiscale CFD simulation of an industrial diameter-transformed fluidized bed reactor with artificial neural network analysis of EMMS drag markers. *Ind Eng Chem Res.* 61(24):8566-8580.